

DNA Repair by Spore Photoproduct Lyase: A Density Functional Theory Study

Jing-Dong Guo, Yi Luo,* and Fahmi Himo*

Theoretical Chemistry, Royal Institute of Technology, ALBANOVA, SE-106 91 Stockholm, Sweden

Received: February 3, 2003; In Final Form: May 21, 2003

Density functional theory calculations using the hybrid functional B3LYP have been performed to probe the energetics of the spore photoproduct lyase (SPL) reactions. This enzyme catalyzes the repair of a thymine dimer caused by UV irradiation of bacterial spore DNA. The calculations support the experimentally suggested mechanism, in which the reaction proceeds through hydrogen atom abstraction from the C6 position of the thymine dimer, followed by β -scission of the C–C bond linking the two bases. The calculations propose, furthermore, that an inter-thymine hydrogen atom transfer step takes place before the back-transfer of the hydrogen atom from the adenosine cofactor. The last step is shown to be the rate-determining step in the reactions.

I. Introduction

The DNA of UV-irradiated bacterial spores accumulates the novel thymine dimer 5-thyminyl-5,6-dihydrothymine (called spore photoproduct, SP), which blocks the normal activity of DNA and can even lead to mutation.¹ Spore photoproduct lyase (SPL) catalyzes the repair of this dimer according to the reaction shown in Scheme 1.²

SPL is an iron–sulfur (FeS) enzyme that uses *S*-adenosyl-methionine (SAM or AdoMet) as a cofactor,³ and it hence belongs to the growing family of FeS/SAM radical enzymes that use the 5'-deoxyadenosyl (5'dAdo) radical, generated from reduction of SAM, in their catalytic processes.⁴ In this family of enzymes, the 5'dAdo radical abstracts a hydrogen atom, which starts the substrate reactions.

On the basis of experiments using a simple bispyrimidine model system, Mehl and Begley proposed the mechanism shown in Scheme 2 for the reactions of SPL.⁵ The 5'dAdo radical initiates the repair by abstracting the C6 hydrogen atom of the spore photoproduct. The C–C bond linking the two pyrimidines, weakened by this hydrogen atom abstraction, undergoes then β -scission. The last step is the transfer of the hydrogen atom back from the 5'dAdo to the thymine monomer, completing the repair.

Recent experiments by Rebeil and Nicholson,⁶ using electrospray ionization mass spectroscopy and HPLC techniques, provided evidence to support the existence of the 5'dAdo radical. Isotope labeling experiments by Cheek and Broderick⁷ gave further support to this mechanism. The spore photoproduct, specifically ³H-labeled at the C6 position, was shown to transfer label to the adenosylmethionine during repair.

In the present study, we use quantum chemical calculations to explore the energetics of the reaction mechanism of Scheme 2. The method employed is the hybrid Hartree–Fock/density functional theory method B3LYP,⁸ which has been used extensively in recent years to study reaction mechanisms of enzymes,⁹ in particular radical-containing enzymes.¹⁰

II. Computational Details

All geometries and energies presented in the present study are computed using the B3LYP⁸ density functional theory method as implemented in the Gaussian98 program package.¹¹

Geometry optimizations were performed using the double- ζ plus polarization basis set 6-31G(d,p). On the basis of these geometries, single-point calculations with the larger basis set 6-311+G(2d,2p) were done for more accurate energies. The spin densities reported are calculated using Mulliken population analysis. Hessians for evaluation of zero-point vibrational effects were calculated at the B3LYP/3-21G level of theory. Solvation energies were added as single-point calculations using the conductor-like solvation model COSMO¹² at the B3LYP/lacvp level, as implemented in the Jaguar program package.¹³ In this model, a cavity around the system is surrounded by a polarizable dielectric continuum. The dielectric constant was chosen to be the standard value used for the protein surroundings, $\epsilon = 4$.

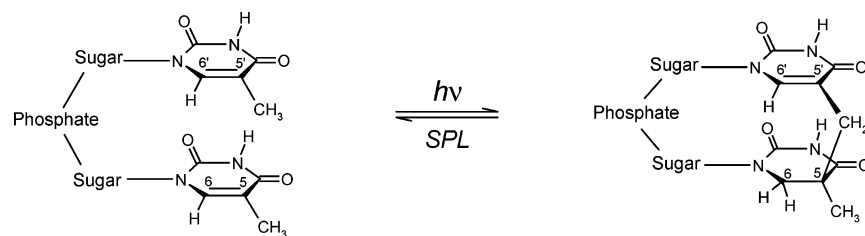
III. Results and Discussion

a. Chemical Models. In any quantum chemical study, it is essential to choose the models to accurately represent the chemical situation. To test one or several reaction pathways and to find the transition states connecting the intermediates, a large number of calculations are usually required. Although the computer power of today allows larger systems to be treated, the models used should not be of the size that this task becomes impractical. In the present work, the largest models consist of as many as 76 atoms, which is quite large considering the high level of theory used.

We modeled the thymine dimer using the two bases and the DNA backbone linking them (two sugars and a phosphate group), as seen in Figures 1–5. In the absence of structural information, the molecule was built in the Spartan software¹⁴ starting from a standard B-form DNA structure. The 5'dAdo was modeled using a ribose ring, where the 2-adenine was replaced by a hydrogen atom, as seen in Figure 1. For future studies, it can be noted that a simple ethane molecule is a fully adequate model of the 5'dAdo, since the active groups in the present reaction are a saturated sp³ carbon and its radical counterpart. The C–H bond strengths of ethane and adenosine are calculated to be quite similar (96.2 and 98.2 kcal/mol, respectively). In the initial phase of the study, this small model was used, and indeed, the energies and transition state structures were very similar to those of the large model.

Finally, one of the oxygens of the phosphate group was protonated in order to obtain a charge-neutral model.

SCHEME 1. Reaction Catalyzed by SPL



SCHEME 2. Proposed Reaction Mechanism of SPL

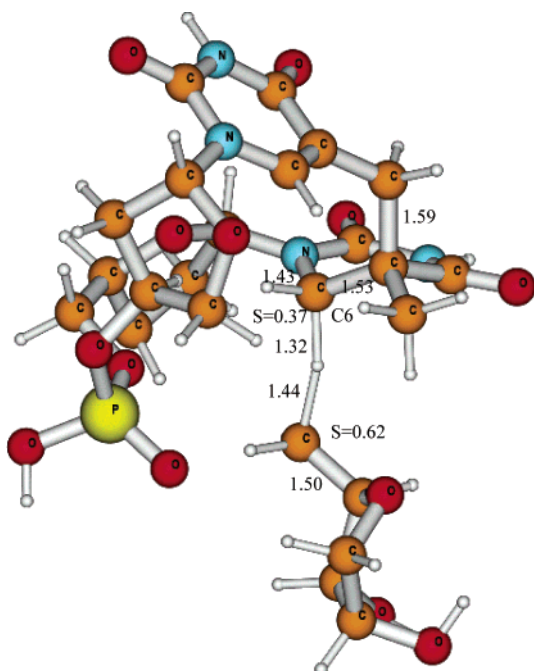
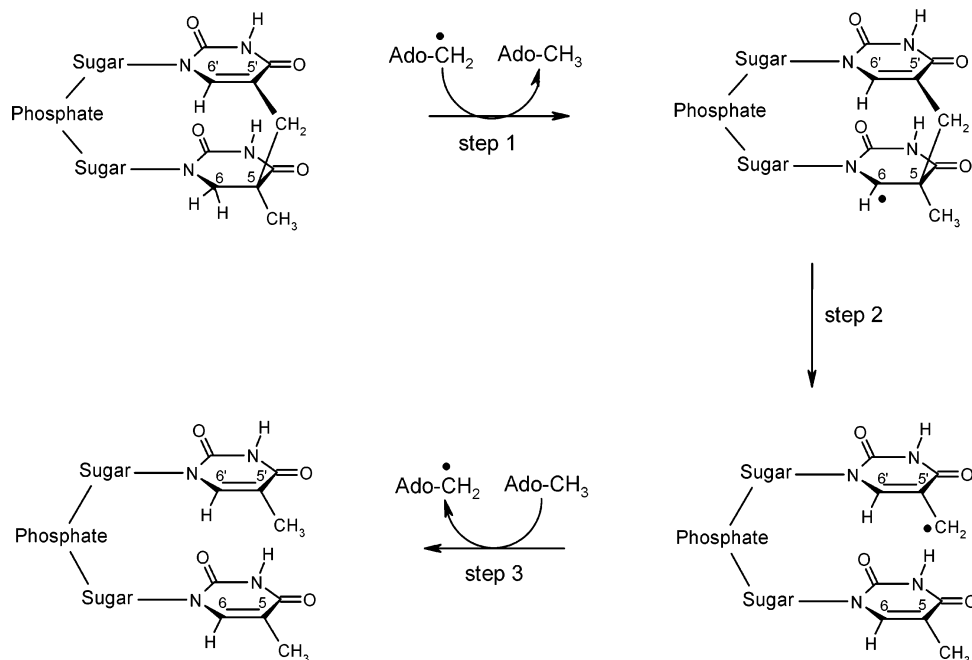


Figure 1. Optimized transition state structure for the hydrogen atom transfer from the thymine dimer to the 5'-dAdo radical (step 1, Scheme 2). Bond lengths are given in angstroms. Major spins are indicated.

b. Creation of the Dimer Radical. We start our discussion at the point where the 5'-dAdo radical is already created. The reduction of AdoMet by an electron from the FeS cluster is

well established experimentally. Furthermore, it is difficult to model accurately with the methods used here, and it requires specific structural and environmental information.

The first step in the substrate reactions is the hydrogen atom abstraction from the C6 position of the thymine dimer by the 5'-dAdo radical. The barrier for this step is calculated to be the quite feasible 14.1 kcal/mol. The step is exothermic by 12.8 kcal/mol, which is the BDE difference between the C-H bond of 5'-dAdo and the C6-H bond of the dimer.

The optimized transition state structure is displayed in Figure 1. The critical C-H bond distances are 1.32 and 1.44 Å. The spin at the transition state is shared between the carbon of the 5'-dAdo (0.62) and the C6 of the dimer (0.37).

c. C-C Bond Cleavage. In the resulting dimer radical intermediate (Figure 2A), the spin is mainly localized at the C6 position. Some spin exists also at the neighboring positions, -0.14 at C5 and 0.08 at the methylene carbon cross-linking the thymines. The bond length of the C-C bond to be broken is 1.60 Å, slightly longer than the C-C single bond in the nonradical species (1.58 Å). We calculate the barrier to break this bond to be the very low 6.2 kcal/mol. Also, this step is exothermic, by 10.8 kcal/mol. At the transition state (Figure 2B), the breaking C-C bond is 2.13 Å. The spin is now distributed over the two thymine rings. After the bond cleavage, the spin is concentrated to one of the rings; see Figure 2C.

The bond scission upon radical creation can be rationalized in terms of hyperconjugation, which is the stabilizing effect caused by the interaction of the singly occupied p-orbital (here localized at the C6 center) with the σ -orbital of the C-C bond

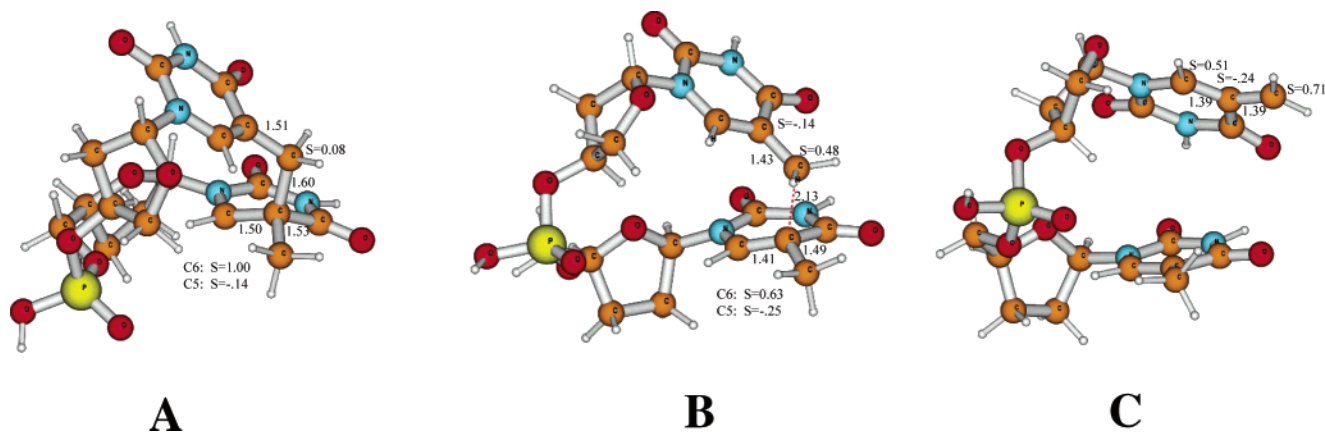


Figure 2. Optimized structures of the dimer radical before the C–C bond cleavage (A), at the transition state (B), and after (C) the C–C bond cleavage (step 2, Scheme 2).

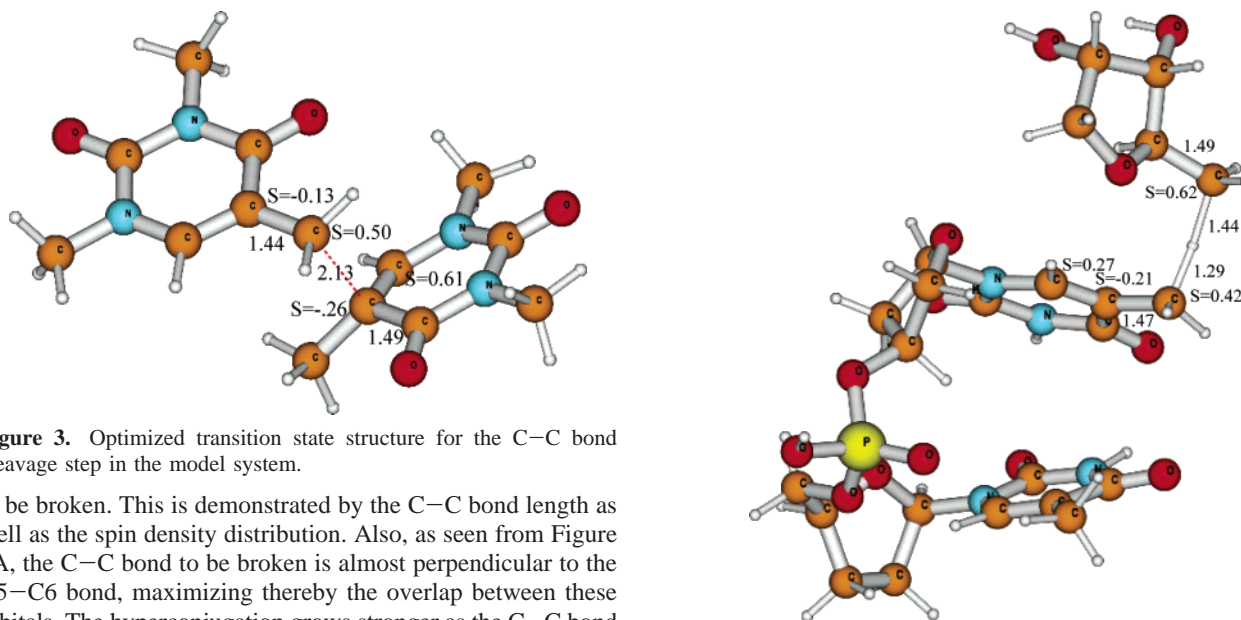


Figure 3. Optimized transition state structure for the C–C bond cleavage step in the model system.

to be broken. This is demonstrated by the C–C bond length as well as the spin density distribution. Also, as seen from Figure 2A, the C–C bond to be broken is almost perpendicular to the C5–C6 bond, maximizing thereby the overlap between these orbitals. The hyperconjugation grows stronger as the C–C bond is broken, hence lowering the barrier for the cleavage.

For comparison, we have also calculated the C–C bond cleavage step in Mehl and Begley's model system.⁵ The optimized transition state structure is shown in Figure 3. The bond lengths and spin distributions are almost identical to those for the transition state of the large system (Figure 2B). For example, the critical C–C bond is also 2.13 Å. The calculated energy barrier is 10.1 kcal/mol, which is ~4 kcal/mol higher than the barrier found for the large system (6.2 kcal/mol). This difference can be understood in terms of ground-state destabilization in the large model. In contrast to the case of the model system, the DNA backbone in the large system prevents the two thymine rings from having optimal positions relative to each other. This effect is bigger in the ground state compared to the transition state, because the C–C bond connecting the two rings is longer in the transition state.

d. Back-Donation of Hydrogen Atom. The final step in the proposed mechanism is the back-transfer of the hydrogen atom from 5'dAdo to the thymine monomer radical, quenching the DNA radical and regenerating the 5'dAdo radical (step 3 in Scheme 2). This step is expected to be energetically unfavorable because the 5'dAdo radical is less stable than the thymine radical. The calculations predict the C–H BDE of 5'dAdo to be 12.2 kcal/mol higher than that for thymine (98.2 vs 86.0 kcal/mol), which means that this step is endothermic by 12.2 kcal/mol. This endothermicity induces a rather high reaction

Figure 4. Optimized transition state structure for the back-transfer of the hydrogen atom (step 3, Scheme 2).

barrier of 23.0 kcal/mol. The optimized transition state structure is shown in Figure 4.

By comparing the position of the 5'dAdo cofactor relative to the DNA when abstracting the hydrogen (Figure 1) and delivering it back (Figure 4), it is difficult to envision how the cofactor can move from one end of the system to the other to affect both hydrogen transfer steps. One possibility could be that the cofactor is located between the two bases, in proximity to both the abstraction and delivery centers. We tried to place it there, but visual inspection showed that it is quite difficult to fit, either between the two bases or in a bridging position where it can reach both centers.

The calculations instead suggest a slightly different path that circumvents this problem. We propose that a hydrogen atom is first transferred from the C5 methyl group of one thymine to the C5' methyl radical of the other, before a hydrogen can be abstracted from 5'dAdo, as displayed in Scheme 3. This way, the 5'dAdo cofactor can remain in the same position relative to the DNA.

The barrier for the almost thermoneutral inter-thymine hydrogen transfer is calculated to be 15.0 kcal/mol, and the transition state structure is shown in Figure 5A. After the transfer (step 3 of Scheme 3) the 5'dAdo cofactor is in a perfect position

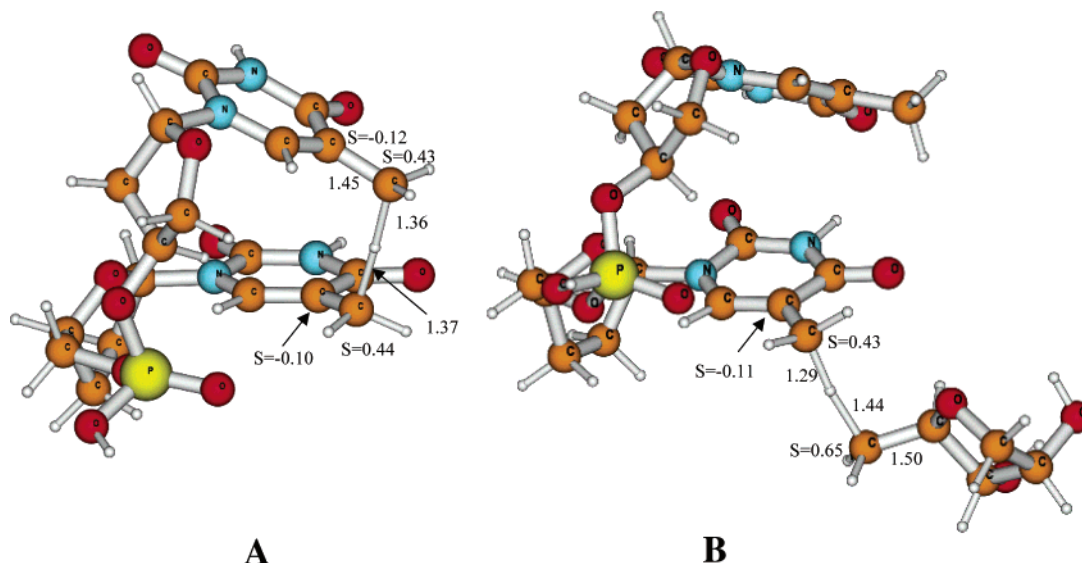
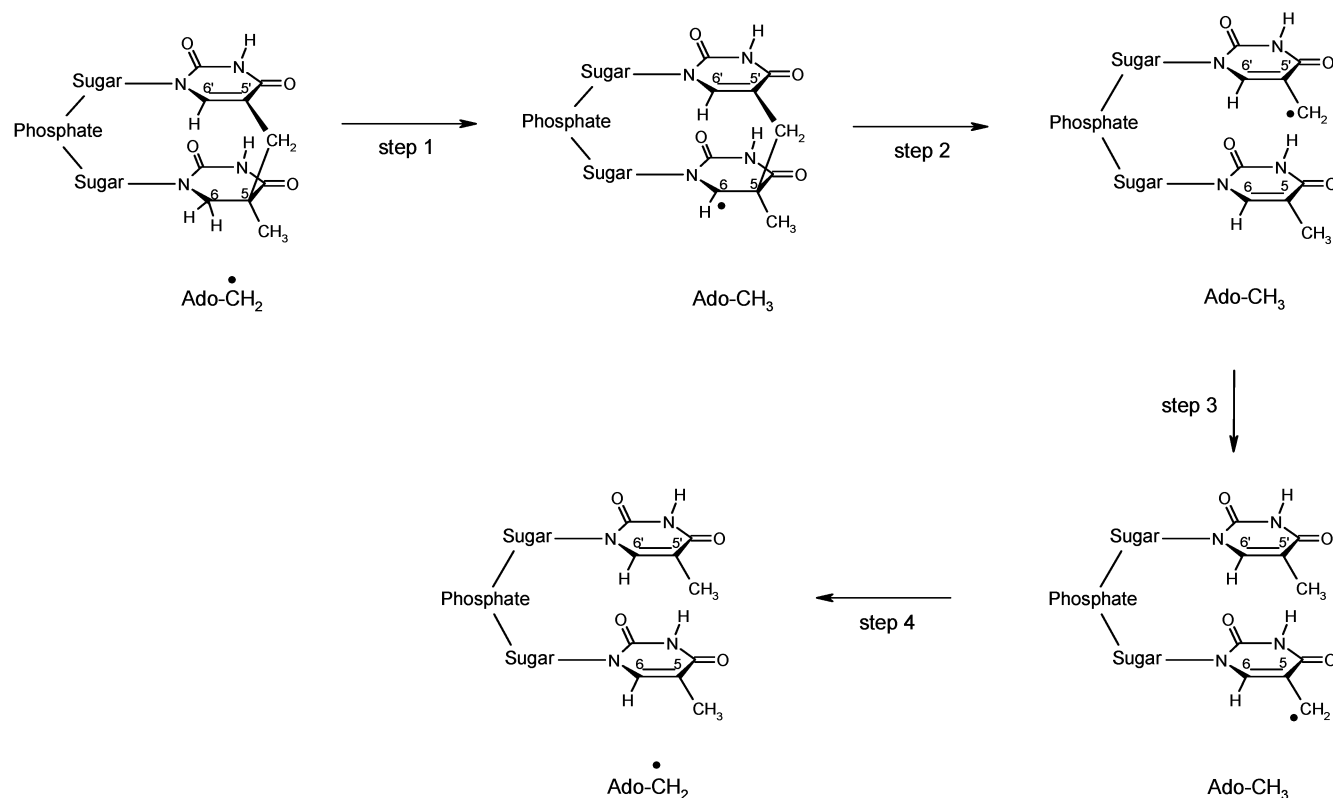


Figure 5. Optimized transition state structures of the inter-thymine hydrogen atom transfer (A) and the back-transfer of the hydrogen atom from adenosine (B).

SCHEME 3. Modified Reaction Mechanism of SPL Proposed in the Present Study



to affect the last step of the reaction (step 4), which is now the back-donation of the hydrogen atom to the C5 methyl.

The energetics of this step are not very different from those obtained for the hydrogen atom transfer to the C5' methyl radical presented above (step 3 of Scheme 2), since the two positions are chemically almost identical. The barrier is calculated to be 24.9 kcal/mol, and the endothermicity, to be 13.5 kcal/mol. The transition state structure is shown in Figure 5B.

The last step is hence the rate-limiting one of the reactions considered here. A barrier of 25 kcal/mol is higher than what can be accepted for enzymatic reactions. From classical transition state theory one can deduce that a barrier of ~18 kcal/mol corresponds to a rate constant of 1 s. For every increase (or

decrease) of 1.4 kcal/mol in the barrier, the rate decreases (or increases) by 1 order of magnitude.

The calculated barrier is believed to be an overestimation because the ground state is overstabilized due to the relatively small model employed, using only two bases of the DNA sequence. In the absence of detailed structural information about the SPL enzyme, these models must be considered as approximate. Another possibility is that this step is coupled to some energetically favorable step following, such as, for instance, the recombination of the Ado radical with the methionine, to regenerate the AdoMet cofactor. Finally, one should not forget that the theoretical methods used here have an inherent error of a few kilocalories per mole.

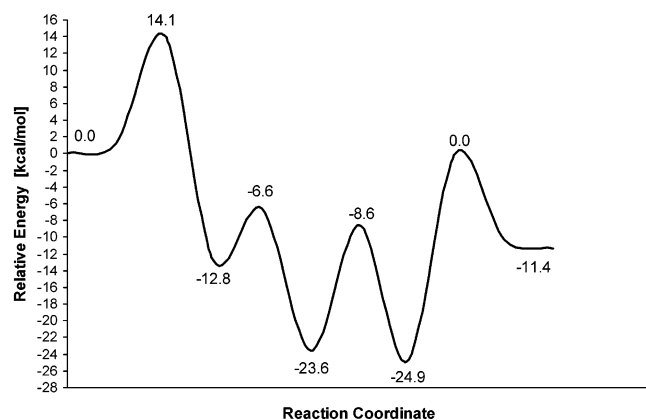


Figure 6. Calculated potential energy surface for the reactions of SPL.

IV. Conclusions

We have in the present paper examined the energetics of the catalytic mechanism of spore photoproduct lyase by means of density functional theory.

We propose that the reactions proceed through the mechanism depicted in Scheme 3. This mechanism differs from the previously proposed one (Scheme 2) in one very important aspect, and that is step 3, where a hydrogen atom is proposed to transfer between the thymine bases. This was invoked to solve the problem of the position of the adenosine cofactor relative to the DNA.

In the preceding steps (steps 1 and 2), the calculations show that the experimentally suggested mechanism is energetically feasible. In particular, the C—C bond cleavage step has a very low barrier, once the dimer radical is created. The rate-limiting step is found to be the hydrogen atom transfer from 5'dAdo to the thymine monomer radical (Scheme 3, step 4), with a quite high calculated barrier of 25 kcal/mol. The calculated potential energy curve for the entire mechanism is shown in Figure 6.

Acknowledgment. F. H. thanks the Wenner-Gren Foundations for financial support. The National Supercomputer Center (NSC) is acknowledged for CPU time.

References and Notes

- (1) (a) Donnellan, J. E.; Setlow, R. B. *Science* **1965**, *149*, 308. (b) Varghese, A. J. *Biochem. Biophys. Res. Commun.* **1970**, *38*, 484.
- (2) (a) Setlow, P. *Annu. Rev. Microbiol.* **1995**, *49*, 29. (b) Munakata, N.; Rupert, C. S. *J. Bacteriol.* **1972**, *111*, 192. (c) Munakata, N.; Rupert, C. S. *Mol. Gen. Genet.* **1974**, *130*, 239. (d) Van Wang, T.-C.; Rupert, C. S. *Photochem. Photobiol.* **1977**, *25*, 123. (e) Fajardo-Cavazos, P.; Salazar, C.; Nicholson, W. L. *J. Bacteriol.* **1993**, *175*, 1735.
- (3) (a) Rebeil, R.; Yubo, S.; Choo-back, L.; Pedraza-Reyes, M.; Kinsland, C.; Begley, T. P.; Nicholson, W. L. *J. Bacteriol.* **1998**, *180*, 4879. (b) Cheek, J.; Krebs, C.; Huynh, B. H.; Broderick, J. B. *J. Inorg. Biochem.* **2001**, *86*, 175.
- (4) Cheek, J.; Broderick, J. B. *J. Biol. Inorg. Chem.* **2001**, *6*, 209.
- (5) Mehl, R. A.; Begley, T. P. *Org. Lett.* **1999**, *1*, 1065.
- (6) Rebeil, R.; Nicholson, W. L. *Proc. Natl. Acad. Sci. U.S.A.* **2001**, *98*, 9038.
- (7) Cheek, J.; Broderick, J. B. *J. Am. Chem. Soc.* **2002**, *124*, 2860.
- (8) (a) Becke, A. D. *Phys. Rev.* **1988**, *A38*, 3098. Becke, A. D. *J. Chem. Phys.* **1993**, *98*, 1372. (b) Becke, A. D. *J. Chem. Phys.* **1993**, *98*, 5648.
- (9) (a) Siegbahn, P. E. M.; Blomberg, M. R. A. *Annu. Rev. Phys. Chem.* **1999**, *50*, 221. (b) Siegbahn, P. E. M.; Blomberg, M. R. A. *Chem. Rev.* **2000**, *100*, 421. (c) Blomberg, M. R. A.; Siegbahn, P. E. M. *J. Phys. Chem. B* **2001**, *105*, 9375.
- (10) Himo, F.; Siegbahn, P. E. M. *Chem. Rev.*, in press.
- (11) Frisch, M. J.; Trucks, G. W.; Schlegel, H. B.; Scuseria, G. E.; Robb, M. A.; Cheeseman, J. R.; Zakrzewski, V. G.; Montgomery, J. A., Jr.; Stratmann, R. E.; Burant, J. C.; Dapprich, S.; Millam, J. M.; Daniels, A. D.; Kudin, K. N.; Strain, M. C.; Farkas, O.; Tomasi, J.; Barone, V.; Cossi, M.; Cammi, R.; Mennucci, B.; Pomelli, C.; Adamo, C.; Clifford, S.; Ochterski, J.; Petersson, G. A.; Ayala, P. Y.; Cui, Q.; Morokuma, K.; Malick, D. K.; Rabuck, A. D.; Raghavachari, K.; Foresman, J. B.; Cioslowski, J.; Ortiz, J. V.; Stefanov, B. B.; Liu, G.; Liashenko, A.; Piskorz, P.; Komaromi, I.; Gomperts, R.; Martin, R. L.; Fox, D. J.; Keith, T.; Al-Laham, M. A.; Peng, C. Y.; Nanayakkara, A.; Gonzalez, C.; Challacombe, M.; Gill, P. M. W.; Johnson, B. G.; Chen, W.; Wong, M. W.; Andres, J. L.; Head-Gordon, M.; Replogle, E. S.; Pople, J. A. *Gaussian 98*, revision A.9; Gaussian, Inc.: Pittsburgh, PA, 1998.
- (12) (a) Barone, V.; Cossi, M. *J. Phys. Chem.* **1998**, *102*, 1995. (b) Barone, B.; Cossi, M.; Tomasi, J. *J. Comput. Chem.* **1998**, *19*, 404.
- (13) *Jaguar 4.2*; Schrodinger, Inc.: Portland, OR, 2000.
- (14) *Spartan 5.0*; Wavefunction, Inc.: Irvine, CA.